Hindawi Publishing Corporation
International Journal of Geophysics
Volume 2013, Article ID 160915, 8 pages
http://dx.doi.org/10.1155/2013/160915

Research Article

Preliminary Results of Marine Electromagnetic Sounding with a Powerful, Remote Source in Kola Bay off the Barents Sea

Valery Grigoryev,[1] Sergey Korotaev,[2,3] Mikhail Kruglyakov,[3,4] Darya Orekhova,[3] Yury Scshors,[3] Evgeniy Tereshchenko,[1] Pavel Tereshchenko,[5] and Igor Trofimov[2]

[1] *Kola Science Centre, Polar Geophysical Institute, Russian Academy of Science, Murmansk, 15 Khalturina Street, Murmansk 183010, Russia*
[2] *Geoelectromagnetic Research Centre of Schmidt Institute of Physics of the Earth, Russian Academy of Sciences, P.O. Box 30, Troitsk, Moscow Region 142190, Russia*
[3] *Kurchatov Institute, Moscow, 1 Akademika Kurchatova Square, Moscow 123182, Russia*
[4] *Moscow State University, Moscow, GSP-1 Leninskie Gory, Moscow 119991, Russia*
[5] *Institute of Terrestrial Magnetism, Ionosphere, and Radiowave Propagation, Russian Academy of Sciences, St. Petersburg Branch, 1 Mendeleevskaya Linia, St. Petersburg 199034, Russia*

Correspondence should be addressed to Darya Orekhova; ordaal@gmail.com

Received 28 September 2012; Accepted 30 December 2012

Academic Editor: Michael S. Zhdanov

We present an experiment conducted in Kola Bay off the Barents Sea in which new, six-component electromagnetic seafloor receivers were tested. Signals from a powerful, remote super-long wave (SLW) transmitter at several frequencies on the order of tens Hz were recorded at the six sites along a profile across Kola Bay. In spite of the fact that, for technical reasons, not all the components were successfully recorded at every site, the quality of the experimental data was quite satisfactory. The experiment resulted in the successful simulation of an electromagnetic field by the integral equation method. An initial geoelectric model reflecting the main features of the regional geology produced field values that differed greatly from the experimental ones. However, step-by-step modification of the original model considerably improved the fit of the fields. Thereby specific features of the regional geology, in particular the fault tectonics, were able to be corrected. These preliminary results open the possibility of inverse problem solving with more reliable geological conclusions.

1. Introduction

Recently marine electromagnetic methods have become a valuable tool for seafloor mapping (e.g., [1, 2]). Among them, methods based on the natural (magnetotelluric) field offer advantages over those based on controlled source electromagnetic methods (CSEM) for lower-crust and upper-mantle mapping, while the latter offer advantages for upper-crust mapping. Although in general terms the audiomagnetotelluric method has been successfully applied to upper-crust survey too, such is not the case for the auroral zone, where the necessary plane-wave condition is roughly violated. A number of types of seafloor electromagnetic receivers measuring four (horizontal electric and magnetic) or five (the same plus vertical magnetic) components of the field, with various types of control sources dropped into the sea have been implemented ([3–8]). However, it is known that measurement of the sixth component (vertical electric) can be of much interest, because it is particularly sensitive to the insulating crust structures ([9]). On the other hand, it can be advantageous to use the powerful stationary control source for land mapping (e.g., [10]) and it is hoped that employment of such a powerful land-based source will also be beneficial in shelf mapping.

In this paper, we present the experiment that made this possibility a reality. The first six-component electromagnetic seafloor receivers have been tested in Kola Bay off the Barents Sea. Signals from a distant, powerful super-long wave (SLW)

transmitter were recorded at six sites along a profile across the bay. The results have been preliminarily interpreted by simulation of the electromagnetic field by the integral equation method.

2. Experiment

This pioneer experiment on seafloor measurements of the electromagnetic field emitted by the powerful land-based SLW transmitter was performed in September 2011. The source represented a grounded horizontal line current (electric bipole) approximately 60 km long located on the Kola Peninsula and oriented along the latitude parallel. The field was emitted at frequencies of 41 Hz, 62 Hz, 82 Hz, and 144 Hz, by 200 A sinusoidal current every fifteen minutes and was measured by the six-component receivers (Figure 1) sited on the floor of the bay. The amplitude of the antenna current was recorded with reference to GPS time.

The receivers were equipped with three orthogonal induction magnetic field sensors with low-noise amplifiers and with three orthogonal electric field sensors. The measured analog signals were received by the six-channel, 16 bit ADC, where they were converted to digital signals and saved for further analysis on a FLASH memory. Accuracy of the conversion was provided by pass-through calibration of the measurement channels using specialized metrology equipment. The receiver technical characteristics are follows.

Frequency range: 0.01 Hz–200 Hz.

Dynamic range of the measured signals: 72 dB.

The magnetic channels sensitivity in frequency band 0.01 Hz–200 Hz: above 0.5 pT at the signal-noise ratio 3/1.

The intrinsic noise of magnetic channels is

1000 fT at $f = 0.1$ Hz,
100 fT at $f = 10$ Hz,
100 fT at $f = 100$ Hz.

The electric channels sensitivity in frequency band 0.01 Hz–200 Hz: above 10 nV/m at the signal-noise ratio 3/1.

Operating depth-up to 500 m.

Before starting and stopping the recording, the verification of high-precision temperature-stabilized receiver clock with GPS time was produced. This ensured data synchronization with the correct time. During each measurement session values of receiver azimuth, roll, and pitch were fixed on a FLASH memory every minute by the receiver orientation unit. The coordinates of the station dive point were fixed by the navigation system of the boat. After measurements the station lifting was performed by the command from the ship through an acoustic channel. The reading of data is carried out after lifting station on the boat. So the antenna current data and the values of the field on the seabed were synchronous.

Figure 1: Six-component seafloor receiver before deployment.

The signal was separated from natural and man-made noise using the spectral analysis of measurement results from Welch's method [11]. As a result, the amplitudes of the six components of the field as well as the phase differences between them were gleaned. The signal-noise ratio for all the components exceeded 30 dB.

As the receiver orientation was random after descent on the floor, the gleaned data needed to be converted into a single-axis coordinate system, taking into account the values of pitch, roll, and yaw of the receiver units.

The new amplitudes of the orthogonal components from the measured ones, A_i and A_k, with phase difference ϕ after turning in one plane with angle ψ, are as follows:

$$\widetilde{A}_i = \sqrt{A_i^2\cos^2\psi - 2A_iA_k\sin\psi\cos\psi\cos\varphi + A_k^2\sin^2\psi},$$
$$\widetilde{A}_k = \sqrt{A_k^2\cos^2\psi + 2A_iA_k\sin\psi\cos\psi\cos\varphi + A_i^2\sin^2\psi}. \quad (1)$$

The new phase difference between them is

$$\widetilde{\varphi} = \varphi + \arcsin\left(\frac{A_k\sin\psi\sin\varphi}{\widetilde{A}_i}\right) + \arcsin\left(\frac{A_i\sin\psi\sin\varphi}{\widetilde{A}_k}\right). \quad (2)$$

To present the measurement results, the Cartesian axis system was used with the x-axis oriented along the geographical meridian facing North and the y-axis oriented along the latitude facing East. The z-axis was oriented vertically, facing up. Calculations (1)–(2) were consequently applied in three planes, taking into account the magnetic declination 14° 56′ E in the area of observations when turning in the XY plane. As a result, we assembled the amplitude values of the field components and the phase differences in a single geographic axis system.

The observation sites were located along two sides of the waterway at a depth of 36 to 85 meters—four on the southern side of the waterway and two on the northern side

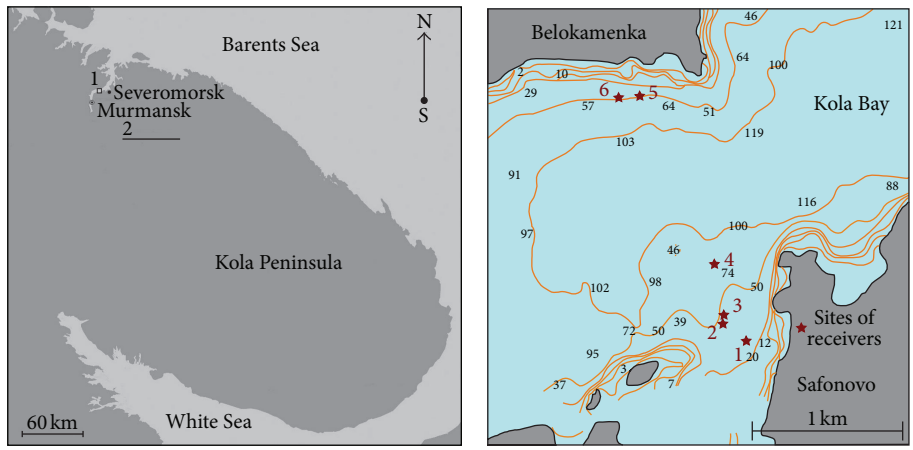

Figure 2: Region of electromagnetic sounding. (a) Area of observations, 1, and the source bipole, 2. (b) Observation sites.

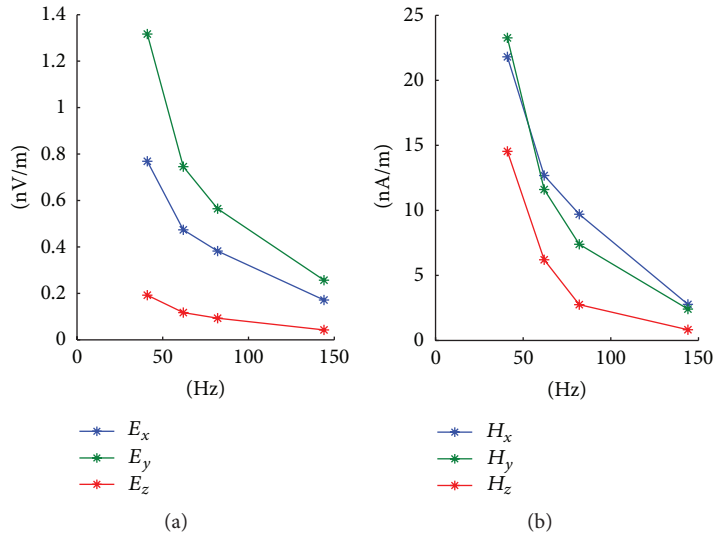

Figure 3: Amplitudes for current reduced to 1 A in the source: (a) electric, V/m and (b) magnetic, A/m components, plotted against frequency, Hz.

(Figure 2) because of the navigation peculiarities in Kola Bay. The receivers were deployed on the seafloor at least thirty minutes before transmission started. The receivers buoyed to the sea surface thirty minutes after transmission stopped.

All of the horizontal and vertical components of the electromagnetic field at all the frequencies were detected at all the observation sites. As a result, data for the magnetic components were obtained at every site except site 3, where the receiver unit had not been fixed on the bay slope and changed its orientation during the session, resulting in noise from the induction sensors. In view of the unreliability of some electric component measurements at sites 2, 5, and 6, electric field data for these sites could not be transformed into a geographical axis system. However, data for single components of the field can be used for interpretation.

Figure 3 presents an example of the plot of the reduced electric (a) and magnetic (b) fields at different frequencies at site 1. The frequency dependence is quite natural.

To take into account the possible space variability of seawater conductivity, we also carried out its vertical and horizontal profiling with an oceanic probe. The conductivity proved to be the same at all the sites of measurement and independent of the depth except for a thin surface layer. It was equal to 3.5 S/m.

3. The Main Features of Regional Geology and the Initial Geoelectric Model

Kola Bay is a submeridional fjord situated on the coast of the Barents Sea in the northwestern part of the Kola

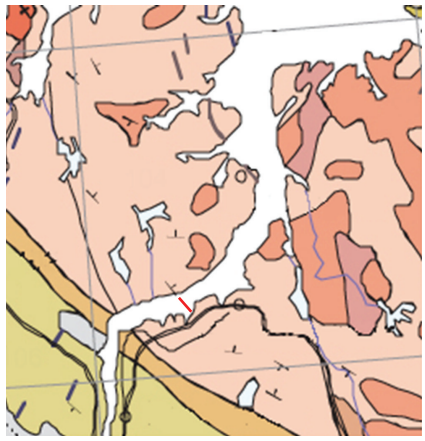

Figure 4: A fragment of the geological map of the Kola Peninsula by Mitrofanov [18]. 92-leucogranites, granodiorites; 102-metavolcanics; 104-granodiorites, tonalites, plagiogranites; 106-micaceous, garnet-mica gneisses. Red line: the observation profile.

Peninsula. Geological and geoelectric description of the area and the fjord itself is given in many works ([12–17]). It passes through two regions: Murmansk Craton and Kola-Norwegian Province, in area of distribution of resistive Archean granitoids and gneisses (a fragment of the geological map by Mitrofanov [18] is given in Figure 4). The average thickness of quaternary sediments (generally glacial and marine) is 50–100 m and reaches 200 m at the entrance of the fjord. In accordance with the cranked curves of the fjord, it is divided into three parts: northern, middle, and southern bends. The northern part is the deepest with depths up to 300 m; in the middle part, where the observation profile is, the depths vary from 35 to 130 m. Kola Bay is also complicated by underwater rapids and branches in the form of bays. The formation of such a complex structure is determined by a system of northwest- and northeast-trending faults, glacial exaration, and irregular postglacial uplift.

On the basis of the publications cited above, the initial geoelectric model was constructed (Figure 5). The background of the model is a two-layered resistive medium: the conductivity of the upper layer is 10^{-4} S/m with a thickness of 2 km; the conductivity of the lower half-infinite layer is 10^{-5} S/m. The conductivity of all the faults is the same, 1 S/m (red in Figure 5); the water conductivity is 3.2 S/m (brown in Figure 5); the sediment conductivity is 1 S/m. The widths of the faults change from 2 to 4 km. The sediments follow the curve of the fjord banks, and their thickness changes from 50 to 200 m at the entrance of the fjord.

4. Method of Simulation

The simulation was based on the 3D integral equation method. The use of this method in electromagnetic geophysics problems is founded on the following model of the complex conductivity distribution. The whole space is

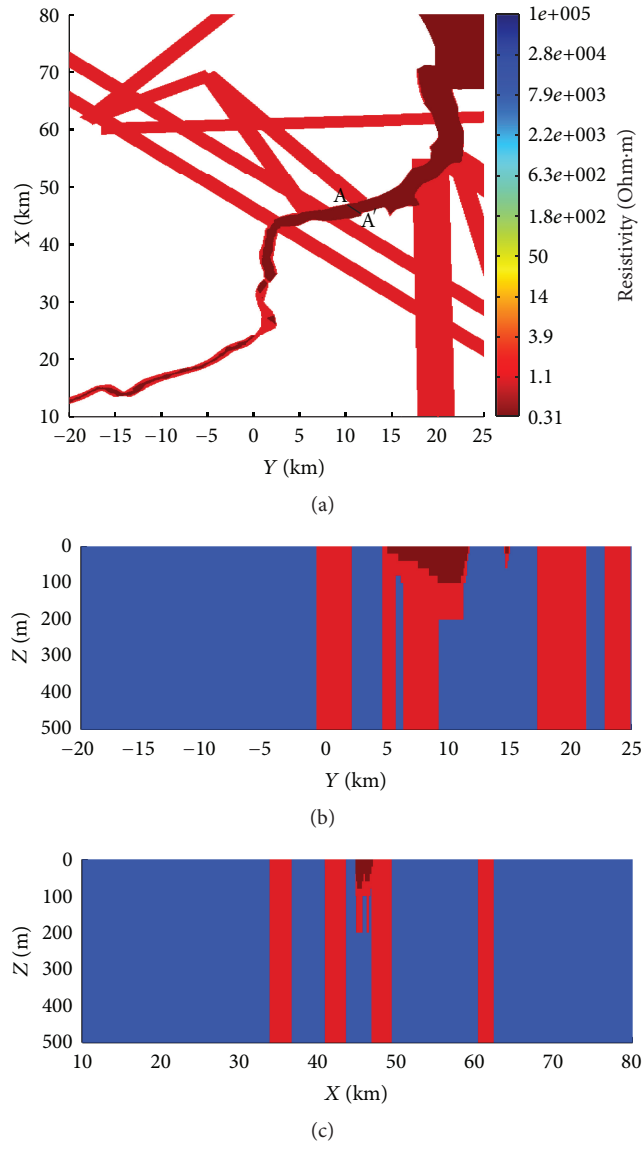

Figure 5: The initial geoelectric model, (a) XY section at $z = 0$ m, (b) YZ section at $x = 45.36$ km, and (c) XZ section at $y = 11.19$ km. The line AA′ represents the profile of observations corresponding to the sites from 5 to 1 in Figure 2(b).

divided into two parts: the normal section and the anomaly. The normal section (background) means the set of unlimited horizontal homogenous layers and two homogeneous half-spaces, where the complex conductivity is constant in each layer and half-space. The conductivity of the upper half-space, which simulates the air, is zero. The anomaly is the 3D volume, where the conductivity is different from that in the normal section. Notice that if we use the integral equation method, we have to specify the conductivity in the whole space. Magnetic permeability is constant μ_0 in the whole space.

If conductivity σ_n of the normal section is defined, the electric and magnetic Green's tensors G_E and G_H can be

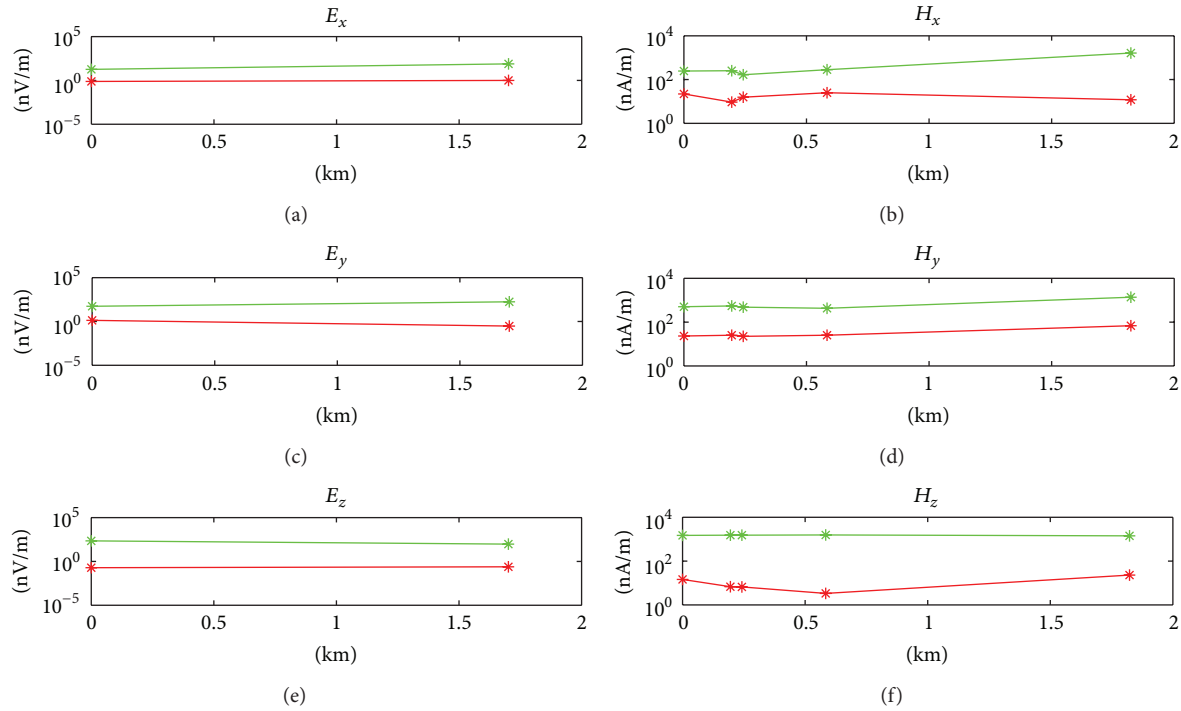

FIGURE 6: Amplitudes of the field components (reduced to 1 A in the source) for the initial geoelectric model at 41 Hz (green lines) as compared with the observed amplitudes (red lines).

computed. This way the following expressions for electrical E and magnetic H fields may be written ([19]):

$$E(M) = i\omega\mu_0 \iiint_V (\sigma_a(M_0) - \sigma_n(M_0)) \times G_E(M, M_0) E(M_0) dV_{M_0} + E_0(M),$$
$$H(M) = i\omega\mu_0 \iiint_V (\sigma_a(M_0) - \sigma_n(M_0)) \times G_H(M, M_0) E(M_0) dV_{M_0} + H_0(M), \quad (3)$$

where ω is the circular frequency, V is the anomalous volume, $\sigma_a(M_0)$ is the anomalous conductivity at the point M_0, and E_0 and H_0 are the primary electrical and magnetic fields. The primary field means the field, which is induced at this point in the normal section by the same source.

If M in the first expression in (3) is inside V, then this expression becomes a 3D singular integral equation of the second kind:

$$E(M) - i\omega\mu_0 \iiint_V (\sigma_a(M_0) - \sigma_n(M_0)) G_E(M, M_0) \times E(M_0) dV_{M_0} = E_0(M). \quad (4)$$

If (4) is solved, its solution E is placed under the integral in (3). Then it becomes possible to compute the electrical and magnetic fields at any point in the space.

The integral equation (4) is solved by the collocation method. The anomalous volume V is divided into the set of rectangular cells V_k, $k = 1, \ldots, N$. The electrical field E is approximated by the constant E^k in V_k, which is the field in the center of V_k. This way we get the following system of linear equations:

$$E^n - i\omega\omega_0 \sum_{k-1}^{N} E^k \iiint_{V_k} (\sigma_a(M_k) - \sigma_n(M_k)) G_E(M, M_0) dV_{M_0} = E_0^n, \quad (5)$$

where M_k is the center of the V_k, $E_0^k = E_0(M_k)$. The system (5) is solved by the generalized minimal residual method.

We start with the very large anomaly extending more than 100 km horizontally in both directions and 2 km in the vertical direction, like the one which was modeled in our previous study ([10]). The computational experiments show that it is not necessary to use that large anomaly, because all the effects in the resulting field are induced by the local objects. These experiments also show that the effects of the geometry of the Kola Bay bottom are very strong, so it is necessary to use the right model of the bathyorography. This way we have to use cells with a very small size: 20 m in the horizontal direction and 5 m in the vertical one. The resulting model consists of 11 million cells. The computations have been conducted on the high-performance computer Skif-Tchebyshev, located at Moscow State University, using fully parallelized 3D forward modeling software PIE3D from the CEMI consortium of the University of Utah.

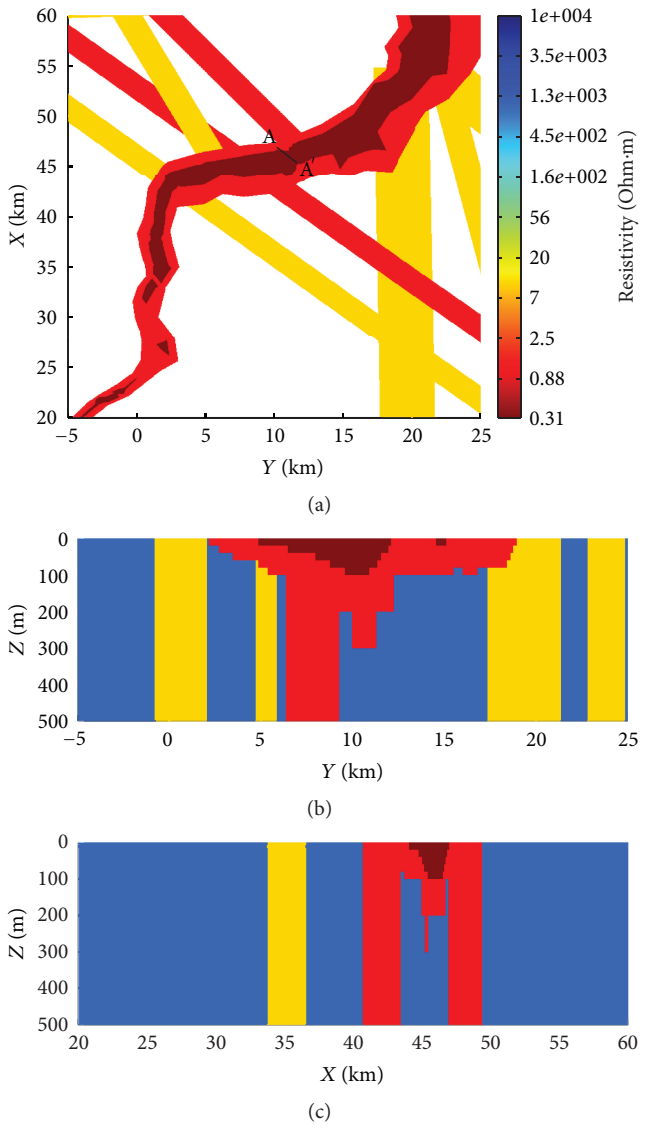

Figure 7: Geoelectric model resulting from trial and error, (a) XY section at $z = 0$ m, (b) YZ section at $x = 45.36$ km, and (c) XZ section at $y = 11.19$ km. The line AA' represents the profile of observations corresponding to the sites from 5 to 1 in Figure 2(b).

5. Preliminary Interpretation

All six components of the field have been computed for the initial geoelectric model (Figure 5). In spite of the fact that there were amplitudes and phases at four frequencies, at the primary stage of investigation we limited ourselves by comparison of the experimental and modeled fields only by the amplitudes and mainly at the lowest frequency. The thing is, phase is too sensitive parameter, which is important at the stage of solving the inverse problem, but which is difficult to employ at the stage of preliminary rough model matching. On the other hand, due to the exposure of an insulating basement around Kola Bay, very thin conductors like bogs or small rivers (which are practically impossible to take into account) strongly influence the field at high frequencies. Therefore at the preliminary rough model matching stage, we pay the most attention to modeling at the most reliable, lowest frequency (41 Hz). Such an approach follows from the experience of land electromagnetic sounding with the same source ([10]).

Table 1

	Average relative misfit at 41 Hz					
	E_x	E_y	E_z	H_x	H_y	H_z
Initial model	58.8146	156.3671	692.1128	28.6447	24.3338	214.7193
Final model	−0.0266	1.6131	2.8070	0.6004	0.4969	−0.3303

When the observed field amplitudes were compared with the computed ones for the initial geoelectric model (Figure 6), it was apparent that they differed widely both by their shape and level (up to three orders of value). Therefore the initial model had to be considerably corrected.

We undertook step-by-step modification of the original model, varying the normal cross section, positions, and conductivity of the faults and geometry of the Kola Bay alluvial belt. Thus, as our original model was rather large and correspondingly every step took considerable time, we also tested the possibility of decreasing the horizontal sizes of the model so that amplitude differences between "large" and "small" models at observation would not exceed about 1%.

We tested a total of about 50 models. One of the best variants is shown in Figures 7 and 8. Of course, the fit of the field components is rather imperfect, but obviously far better than in Figure 6. The average relative misfits for the EM-field amplitudes at 41 Hz are presented in Table 1. At frequencies of 62 and 82 Hz, the fit is only slightly worse than that presented in Figure 8 at 41 Hz and evidently departs from fit only at the highest frequency, 144 Hz.

Thus the model presented in Figure 7 can be a good starting point for strict solving of the inverse problem. Although this model is not final, it allows the inference of some qualitative geophysical and geological conclusions.

(i) The normal cross section attained an order of magnitude more conductive than it was believed before.

(ii) Kola Bay is surrounded by a sedimentary alluvial belt. Evidently it is the result of regional postglacial uplift. The sedimentary belt proved to be asymmetric in accordance with normal right displacement of the ancient river.

(iii) Conductivity of the faults proved essentially different. Probably the larger conductivity of a couple of faults seen in Figure 7 is related to contemporary tectonic activity.

6. Conclusions

This pioneer experiment with a new six-component electromagnetic seafloor receiver and with a distant, powerful SLW transmitter was carried out in Kola Bay off the Barents Sea. The receivers were deployed at six sites along a profile across the bay. Not all six components were successfully

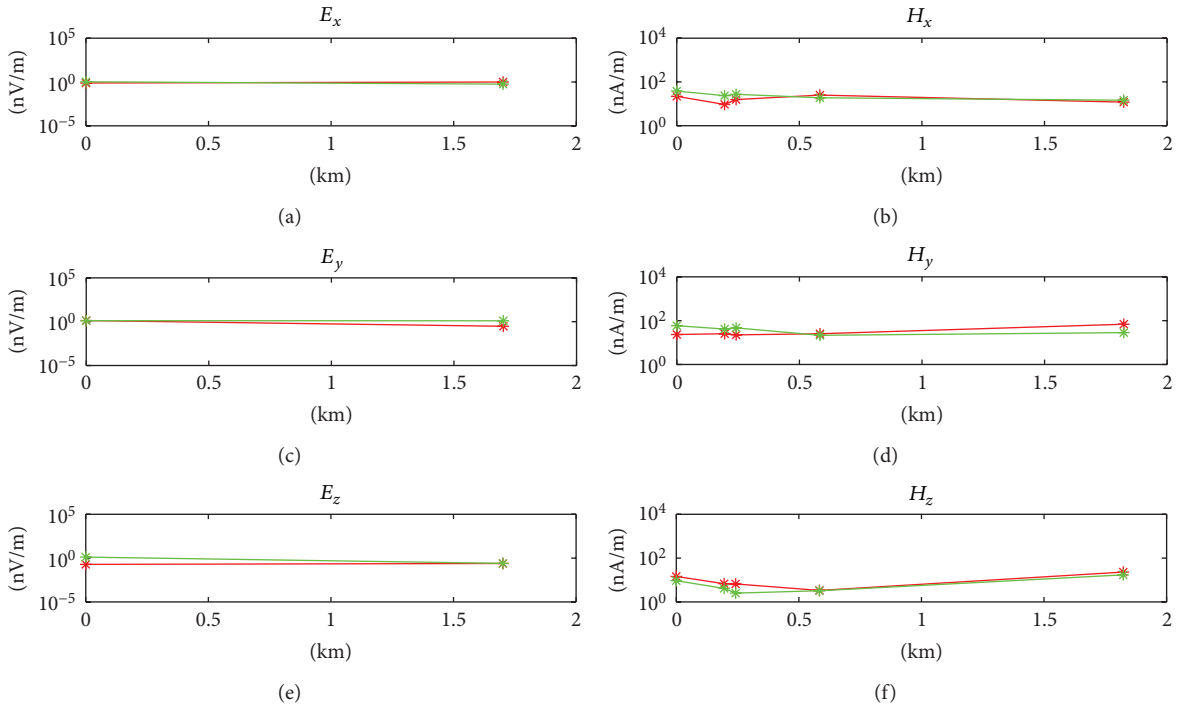

Figure 8: Amplitudes of the field components (reduced to 1 A in the source) for geoelectric model resulting from trial and error at 41 Hz (green lines) as compared with the observed amplitudes (red lines).

measured at all the sites in particular, due to the mechanical unreliability of electric antennas. Nevertheless, the quality of the experimental data turned out to be quite satisfactory.

The data have been preliminarily interpreted by a trial-and-error method with simulation of the electromagnetic field by an integral equation method. The resulting geoelectric model differs from the initial one, and this difference reveals new features of regional geology, in particular of fault tectonics. The resulting model is also the appropriate starting point for strict solving of the inverse problem with subsequently more comprehensive geological interpretation.

Acknowledgments

The work was supported by RFBR (Grant 11-05-12015). The authors acknowledge the University of Utah's Consortium for Electromagnetic Modeling and Inversion (CEMI) for providing 3D forward modeling software PIE3D.

References

[1] K. Key, "Marine electromagnetic studies of seafloor resources and tectonics," *Surveys in Geophysics*, vol. 33, no. 1, pp. 135–167, 2011.

[2] K. A. Weitemeyer, S. Constable, and A. M. Tréhu, "A marine electromagnetic survey to detect gas hydrate at Hydrate Ridge, Oregon," *Geophysical Journal International*, vol. 187, pp. 45–62, 2011.

[3] R. L. Evans, M. C. Sinha, S. C. Constable, and M. J. Unsworth, "On the electrical nature of the axial melt zone at 13∘N on the East Pacific Rise," *Journal of Geophysical Research B*, vol. 99, no. 1, pp. 577–588, 1994.

[4] S. Constable and C. S. Cox, "Marine controlled-source electromagnetic sounding 2. The PEGASUS experiment," *Journal of Geophysical Research B*, vol. 101, no. 3, pp. 5519–5530, 1996.

[5] L. MacGregor and M. Sinha, "Use of marine controlled-source electromagnetic sounding for sub-basalt exploration," *Geophysical Prospecting*, vol. 48, no. 6, pp. 1091–1106, 2000.

[6] L. MacGregor, M. Sinha, and S. Constable, "Electrical resistivity structure of the Valu Fa Ridge, Lau Basin, from marine Controlled-Source electromagnetic sounding," *Geophysical Journal International*, vol. 146, no. 1, pp. 217–236, 2001.

[7] S. Ellingsrud, T. Eidesmo, S. Johansen, M. C. Sinha, L. M. MacGregor, and S. Constable, "Remote sensing of hydrocarbon layers by seabed logging (SBL): results from a cruise offshore Angola," *Leading Edge*, vol. 21, no. 10, pp. 972–982, 2002.

[8] M. C. Sinha, P. D. Patel, M. J. Unsworth, T. R. E. Owen, and M. R. G. Maccormack, "An active source electromagnetic sounding system for marine use," *Marine Geophysical Researches*, vol. 12, no. 1-2, pp. 59–68, 1990.

[9] M. N. Berdichevsky, O. N. Zhdanova, and M. S. Zhdanov, *Marine Deep Geoelectrics*, Nauka, Moscow, Russia, 1989.

[10] E. P. Velikhov, V. F. Grigor'v, M. S. Zhdanov et al., "Electromagnetic sounding of the Kola Peninsula with a powerful extremely low frequency source," *Doklady Earth Sciences*, vol. 438, no. 1, pp. 711–716, 2011.

[11] F. J. Harris, "On the use of windows for harmonic analysis with the discrete Fourier transform," *Proceedings of the IEEE*, vol. 66, no. 1, pp. 51–83, 1978.

[12] E. P. Velikhov, Ed., *Geoelectrical Studies with a Powerful Current Source on the Baltic Shield*, Nauka, Moscow, Russia, 1989.

[13] A. A. Kovtun, S. A. Vagin, I. L. Vardanjants, E. L. Kokvina, and N. I. Uspenskiy, "Magnetotelluric study of the structure of the crust and mantle of the eastern part of the Baltic Shield," *Izvestiya—Physics of the Solid Earth*, no. 3, pp. 32–36, 1994.

[14] A. A. Zhamaletdinov, "Graphite in the Earth's crust and electrical conductivity anomalies," *Izvestiya—Physics of the Solid Earth*, vol. 32, no. 4, pp. 272–288, 1996.

[15] L. L. Vanjan and N. I. Pavlenkova, "Layer of low velocity and high electrical conductivity at the base of the upper crust of the Baltic Shield:," *Izvestiya—Physics of the Solid Earth*, no. 1, pp. 37–45, 2002.

[16] E. V. Spiridonov, *Paleoseismodislocations on the coast of the Barents Sea [Ph.D. thesis]*, MSU, Moscow, Russia, 2007.

[17] E. A. Kovalchuk and E. V. Shipilov, "The first data about the structure and lithology of the section of the Kola Fjord sediments," in *Proceedings of the International Scientific Conference on the 100th Anniversary of D. G. Panov*, pp. 157–160, SSC Academy of Sciences, Rostov-on-Don, Russia, 2009.

[18] F. P. Mitrofanov, Ed., *Geological Map of the Kola Region*, Scale 1:500000. 2001. Apatity.

[19] M. S. Zhdanov, *Geophysical Inverse Theory and Regularization Problems*, Elsevier, Amsterdam, The Netherlands, 2002.